Astroparticle Physics with AMS-02*

A. G. Malinin**
(on behalf of the AMS Collaboration)

Institute for Physical Science and Technology, University of Maryland, USA

Received January 20, 2004

Abstract—The main physics goals of the AMS-02 experiment in the astroparticle domain are searches for antimatter and dark matter. The discovery potential of primordial antimatter by AMS-02 is presented, emphasizing the completeness of the AMS-02 detector for these searches. Meanwhile, antiproton detection suffers from a large secondary interaction background; the anti-^{4}He or anti-^{3}He signal would allow one to probe the Universe for existence of antimatter. The expected signal in AMS-02 is presented and compared to results from present experiments. The e^+ and antiproton channels will contribute to the dark matter detection studies. A SUSY neutralino candidate is considered. The expected flux sensitivities in a three-year exposure for the e^+/e^- ratio and antiproton yields as a function of energy are presented and compared to other direct and indirect searches.

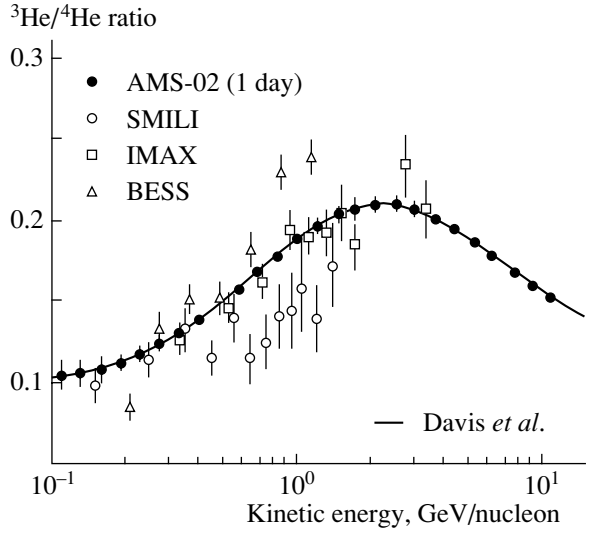

Fig. 1. Example of expected AMS-02 single-day ^{3}He/^{4}He ratio measurement.

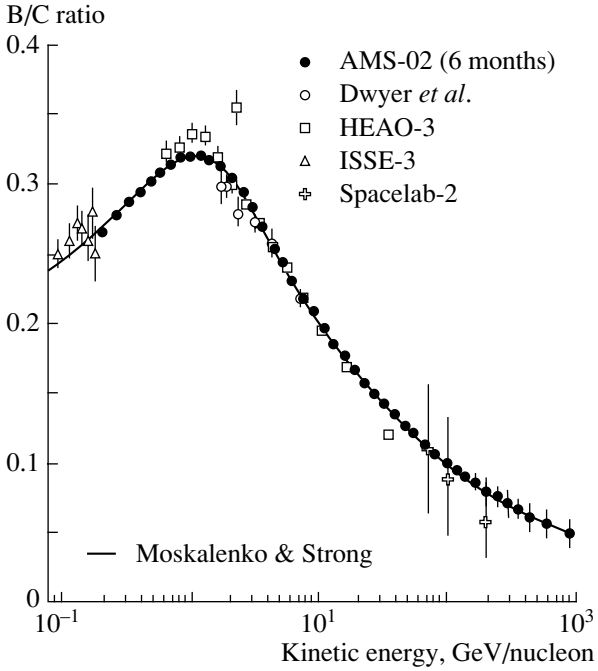

Fig. 2. Example of expected AMS-02 B/C ratio 6-month measurements.

antiprotons) or structures (in case of positrons) to be seen in the otherwise predictable cosmic-ray spectra. Considering the hypothesis of a possible clumpy DM, the expected fluxes of such primary positrons or antiprotons may be enhanced since the annihilation rate is proportional to the squared DM density [15], contrary to direct DM searches, which will suffer from a decreased probability for the Earth to be contained in an eventual DM clump.

Studying the primary and secondary cosmic-ray fluxes and energy distributions is not only a necessary step to understand the backgrounds on top of which a signal of "new physics" is expected, but also allows one to extract information on their transport history and on the nature and distribution of their sources [16]. A better understanding of the spectra of protons and He, which dominate the cosmic-ray abundance, is also important for atmospheric-neutrino flux calculations [17]. ^{3}He/^{4}He, B/C, and sub-Fe/Fe ratios allow one to measure the mean ISM density in the Galaxy crossed by a cosmic ray (the current measurement gives 9 g cm^{-2}). The ^{10}Be isotope with a half-life of 1.6×10^6 yr is the most important radioactive clock for measuring the age of cosmic rays. The ratio of radioactive ^{10}Be to stable ^{9}Be is sensitive to the propagation lifetime of cosmic rays and not to the total amount of matter traversed.

AMS-02 EXPERIMENT CAPABILITIES

A Monte Carlo physics performance study using the general AMS-02 computer model, based on the GEANT3 [18] and GEANT4 [19] simulation packages, was carried out. The calculated cosmic ray (CR) and background fluxes take into account the predicted geomagnetic conditions during the AMS-02 mission on the ISS. The simulated performance of AMS subdetectors was checked against the AMS flight and prototype test beam data and found to be in good agreement with them. Finally, more than 10^9 events containing $p^{\pm}$, He, $e^{\pm}$, and other CR particles at different energies have been fully simulated passing through the detector and then reconstructed. For every particular physics channel, the selection criteria were defined in order to separate the signal from background particles, and the expected number of signal events for the AMS-02 mission was obtained. Thanks to its large geometrical acceptance of about 1 m^2 sr, a high magnetic spectrometer resolving power of $BL^2 = 0.9$ T m^2, and three-year-long exposure time, AMS-02 will identify and measure over 10^9 protons with energies above 100 MeV, and 10^8 He, $10^5(10^4)$ carbon (boron) with energies above 100 MeV/nucleon. Light isotope separation based on velocity (RICH detector) and momentum measurement will be possible up to 10 GeV/nucleon.

In Figs. 1–3, the resulting expected AMS-02 measurements of the ^{3}He/^{4}He, B/C, and ^{10}Be/^{9}Be ratios are shown together with the present data and theoretical CR propagation from the leaky box (LBM) and diffusive halo (DHM) model predictions.

The MC results clearly show that AMS-02 will have a high potential to study beryllium as well as

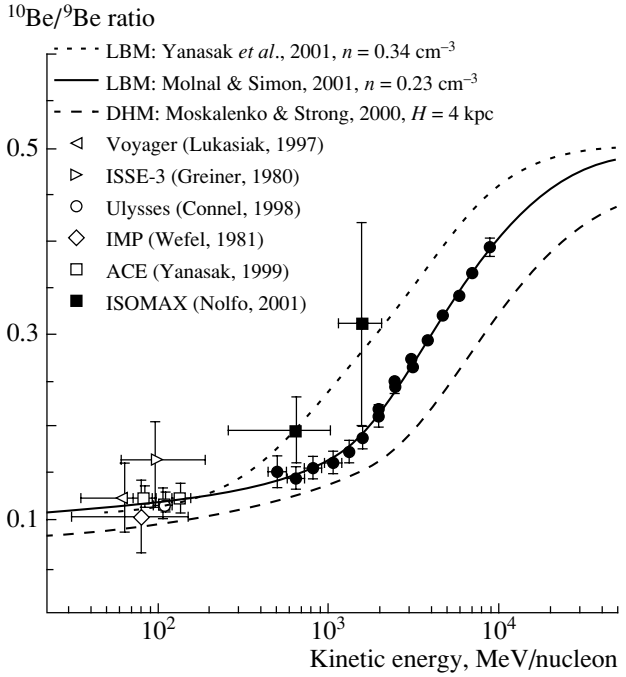

Fig. 3. AMS-02 ^{10}Be/^{9}Be ratio 6-month measurement potential. Closed circles are AMS-02 expectations.

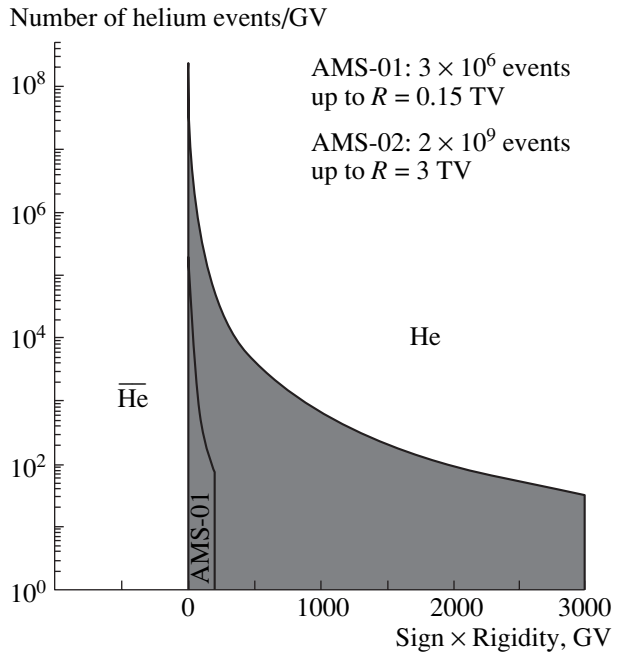

Fig. 4. The expected AMS-02 3-yr cosmic-ray helium spectra measurement compared to AMS-01 results.

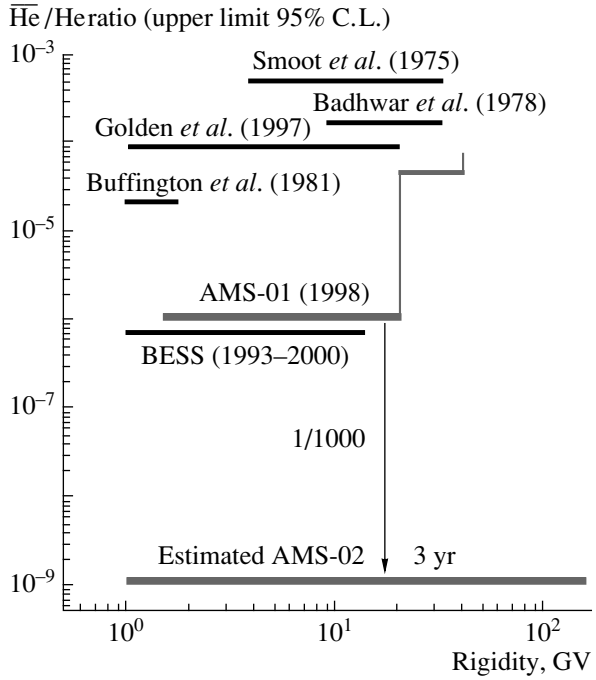

Fig. 5. The expected AMS-02 antihelium/helium flux ratio upper limit at 95% C.L.

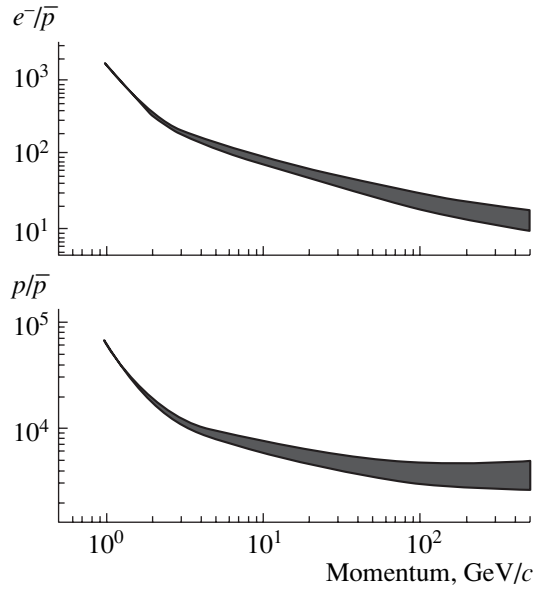

Fig. 6. Electron and proton backgrounds to antiproton signal ratios.

other isotopes in CR up to iron with unmatched precision measurements of the element abundances and the isotopic ratios. The CR propagation models will benefit from accurate AMS-02 data, which in turn will decrease the theoretical uncertainties for "new physics" signals.

The search for antimatter (anti-helium and heavier antinuclei) requires the capability to identify a charged particle and to measure its absolute rigidity value and the sign of its electric charge with the

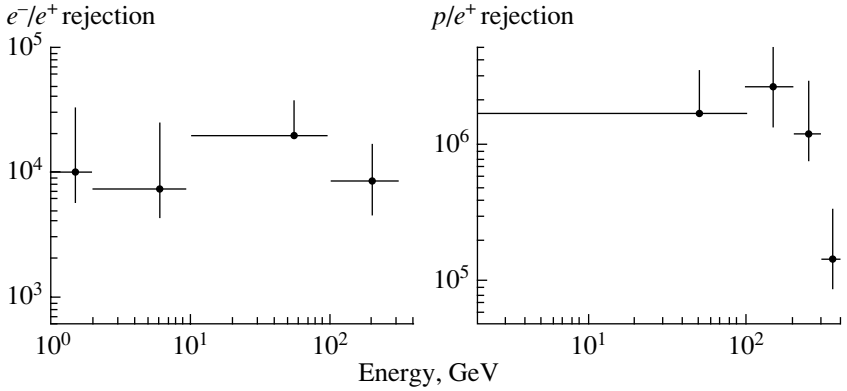

Fig. 7. The obtained e^+ rejection as a function of particle momentum against electrons (left panel) and protons (right panel).

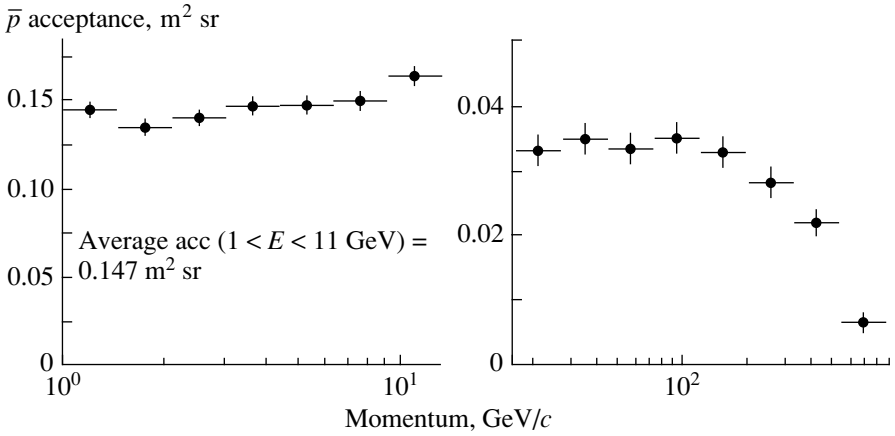

Fig. 8. The estimated average low-energy (left panel) and full range (right panel) AMS-02 antiproton acceptance after all cuts have been applied.

highest possible degree of confidence. A combined analysis based on AMS-02 redundant particle identification and a precise Silicon Tracker rigidity measurement allowed one to achieve over 10^9 background rejection power for the anti-helium signal. The corresponding measured spectra and anti-helium flux upper limit are shown in Figs. 4 and 5 together with the AMS-01 data and present limits.

The searches for DM signals in the antiproton and positron channels suffer from huge proton and electron backgrounds. To get the identification purity of the antiproton and positron samples equal to a few percent, an $O(10^4)$ to $O(10^6)$ background rejection level should be obtained (Fig. 6). To partly remove the proton background from positron signal, the TRD was used. The obtained TRD electron/hadron rejection ranged from 10^3 for 10-GeV and 10^2 for 300-GeV protons. Vetoing events with additional "hits" in the AMS-02 subdetectors in the vicinity of the reconstructed particle trajectory effectively removed the bulk of the interacted background. To discriminate positrons from protons and antiprotons from electrons at low energy, the AMS-02 RICH velocity measurement was used for particles with momentum less than 12.5 GeV/c. At higher energy, to further reduce the proton background, a 3D analysis of the ECAL energy distribution was done. Finally, the residual electron and/or proton background was removed by matching the energy deposition in the ECAL and the rigidity measured by Tracker. Figures 7 and 8 show the obtained background rejection against electrons and protons for a positron signal and AMS-02 antiproton acceptance after all cuts have been applied [20].

Figure 9 shows the simulation of the AMS-02 three-year high-statistics measurement of the cosmic antiproton spectrum up to 400 GeV and the residual background. In Fig. 10, an example of the AMS-02 antiproton flux measurement is shown together with the present experimental data compared to the various models of the secondary antiproton spectrum. The energy region around 10 GeV has less model

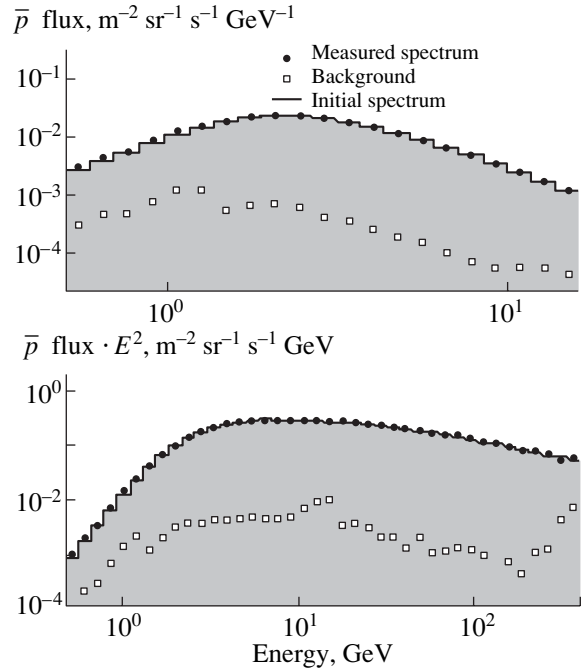

Fig. 9. Example of the AMS 3-yr combined measurement of the cosmic antiproton spectrum and residual background.

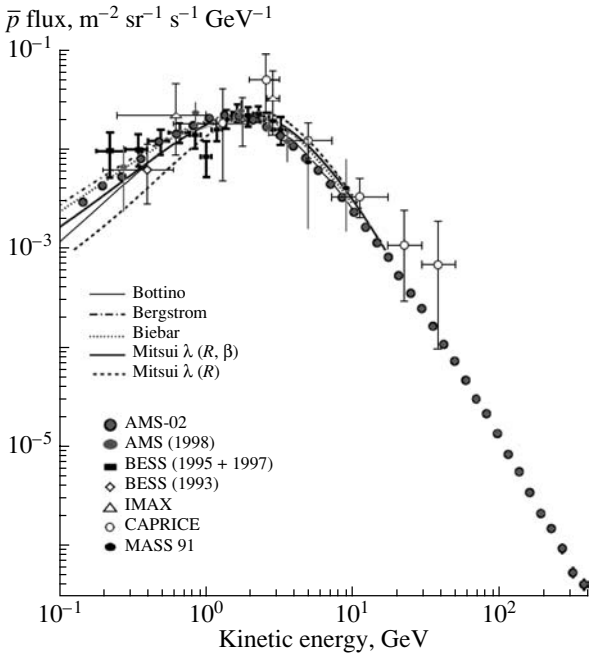

Fig. 10. Present cosmic-ray antiproton flux measurements together with an example of AMS-02 3-yr measurement.

dependence and looks more promising for possible DM related deviation searches.

The positron energy estimation was done by using

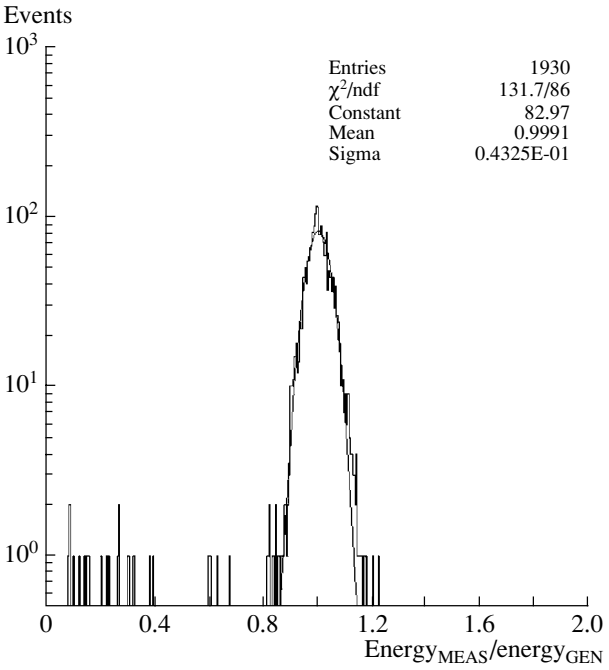

Fig. 11. MC prediction for the AMS-02 positron energy resolution function.

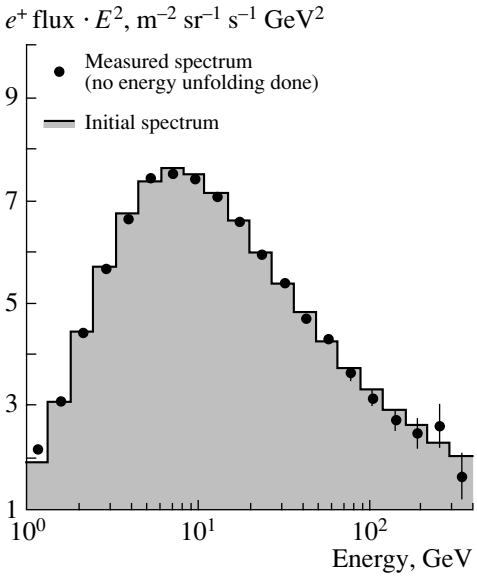

Fig. 12. Example of the AMS-02 3-yr combined measurement of the cosmic e^+ spectrum.

combined ECAL energy and Tracker rigidity quantities. Figure 11 shows the reconstructed energy resolution for 16-GeV positrons. An example of the positron expected spectrum is shown in Fig. 12 up to 400 GeV and without energy unfolding. The resulting spectrum was used to estimate the accuracy of the projected AMS-02 cosmic positron fraction measurement (less model-dependent value compared

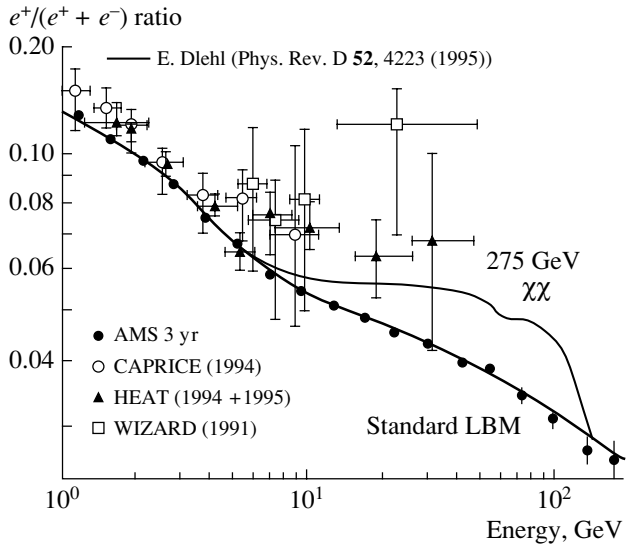

Fig. 13. Present cosmic positron fraction measurements and estimated 3-yr AMS-02 measurement. Solid lines are one of the most favorable SUSY scenarios and the standard LBM prediction.

to the positron flux). The result is shown in Fig. 13 together with the LBM prediction and one of the most favorable theoretical scenarios with a bump structure formed by the primary positrons originated from the annihilations of the SUSY neutralino DM candidate. The present cosmic-positron fraction-ratio measurements are generally compatible with a secondary origin; however, large uncertainties associated with the measurements do not allow one to exclude a primary positron component.

CONCLUSION

During the three-year mission in space, AMS-02 will perform precise, high-statistics cosmic-ray measurements in the fraction of GeV to few-TeV energy range. It will advance our knowledge of astroparticle physics phenomena and will have a high discovery potential of cosmic nuclear antimatter and dark matter.

REFERENCES

1. G. M. Viertel and M. Capell, Nucl. Instrum. Methods Phys. Res. A **419**, 295 (1998).
2. J. Alcaraz *et al.*, Nuovo Cimento A **112**, 1325 (1999).
3. D. Alvisi *et al.*, Nucl. Instrum. Methods Phys. Res. A **437**, 212 (1999).
4. J. Alcaraz *et al.*, Phys. Lett. B **461**, 387 (2000).
5. J. Alcaraz *et al.*, Phys. Lett. B **472**, 215 (2000).
6. J. Alcaraz *et al.*, Phys. Lett. B **484**, 10 (2000).
7. J. Alcaraz *et al.*, Phys. Lett. B **490**, 27 (2000).
8. G. F. Smoot *et al.*, Phys. Rev. Lett. **35**, 258 (1975).
9. G. Steigman *et al.*, Annu. Rev. Astron. Astrophys. **14**, 339 (1976).
10. G. Badhwar *et al.*, Nature **274**, 137 (1978).
11. A. Buffington *et al.*, Astrophys. J. **248**, 1179 (1981).
12. R. L. Golden *et al.*, Astrophys. J. **479**, 992 (1999).
13. J. F. Ormes *et al.*, Astrophys. J. Lett. **482**, L187 (1997).
14. T. Saeki *et al.*, Phys. Lett. B **422**, 319 (1998).
15. E. A. Baltz *et al.*, Phys. Rev. D **65**, 063511 (2002).
16. I. V. Moskalenko and A. W. Strong, Adv. Space Res. **27**, 717 (2001).
17. T. K. Gaiser, T. Stanev, *et al.*, Phys. Rev. D **54**, 5578 (1996).
18. R. Brun *et al.*, GEANT3, CERN-DD/EE/84-1 (Revised 1987).
19. S. Agistinelli *et al.* (GEANT4 Collab.), Nucl. Instrum. Methods Phys. Res. A **506**, 250 (2003).
20. V. Choutko, G. Lamanna, A. Malinin, and E. S. Seo, Int. J. Mod. Phys. A **17**, 1817 (2002).